Accepted Manuscript

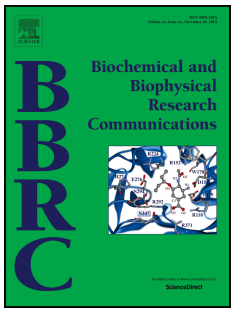

The role of plasmin in the pathogenesis of murine multiple myeloma

Salita Eiamboonsert, Yousef Salama, Hiroshi Watarai, Douaa Dhahri, Yuko Tsuda, Yoshio Okada, Koichi Hattori, Beate Heissig

PII: S0006-291X(17)30924-5

DOI: 10.1016/j.bbrc.2017.05.062

Reference: YBBRC 37783

To appear in: *Biochemical and Biophysical Research Communications*

Received Date: 3 May 2017

Accepted Date: 10 May 2017

Please cite this article as: S. Eiamboonsert, Y. Salama, H. Watarai, D. Dhahri, Y. Tsuda, Y. Okada, K. Hattori, B. Heissig, The role of plasmin in the pathogenesis of murine multiple myeloma, *Biochemical and Biophysical Research Communications* (2017), doi: 10.1016/j.bbrc.2017.05.062.

BBRC, original manuscript

3859 words

The role of plasmin in the pathogenesis of murine multiple myeloma

Salita Eiamboonsert[a], Yousef Salama[a], Hiroshi Watarai[b], Douaa Dhahri[a], Yuko Tsuda[c], Yoshio Okada[b], Koichi Hattori[b,d,*], Beate Heissig[a,e,*,†]

[a] Division of Stem Cell Dynamics, Center for Stem Cell Biology and Regenerative Medicine, The Institute of Medical Science, The University of Tokyo, 4-6-1 Shirokanedai, Minato-ku, Tokyo 108-8639, Japan
[b] Center for Stem Cell biology and Regenerative Medicine, The Institute of Medical Science, The University of Tokyo, 4-6-1 Shirokanedai, Minato-ku, Tokyo 108-8639, Japan
[c] Faculty of Pharmaceutical Sciences, Kobe Gakuin University, 1-1-3 Minatojima, Chuo-ku, Kobe 850-8586, Japan.
[d] Center for Genome and Regenerative Medicine, Juntendo University School of Medicine, 2-1-1 Hongo, Bunkyo-ku, Tokyo 113-8421, Japan
[e] Atopy Center, Juntendo University School of Medicine, 2-1-1 Hongo, Bunkyo-ku, Tokyo 113-8421, Japan
[*] Equally contributed senior authors
[†] Corresponding author

Address correspondence to:

Beate Heissig, MD
Division of Stem Cell Dynamics, The Institute of Medical Science,
The University of Tokyo
4-6-1, Shirokanedai, Minato-ku,
Tokyo 108-8639, JAPAN.
Phone: +81-3-5449-5136,
Fax: +81-3-5449-5724,
E-mail: heissig@ims.u-tokyo.ac.jp

Abstract

Aside from a role in clot dissolution, the fibrinolytic factor, plasmin is implicated in tumorigenesis. Although abnormalities of coagulation and fibrinolysis have been reported in multiple myeloma patients, the biological roles of fibrinolytic factors in multiple myeloma (MM) using *in vivo* models have not been elucidated. In this study, we established a murine model of fulminant MM with bone marrow and extramedullar engraftment after intravenous injection of B53 cells. We found that the fibrinolytic factor expression pattern in murine B53 MM cells is similar to the expression pattern reported in primary human MM cells. Pharmacological targeting of plasmin using the plasmin inhibitors YO-2 did not change disease progression in MM cell bearing mice although systemic plasmin levels was suppressed.

Our findings suggest that although plasmin has been suggested to be a driver for disease progression using clinical patient samples in MM using mostly *in vitro* studies, here we demonstrate that suppression of plasmin generation or inhibition of plasmin cannot alter MM progression *in vivo*.

Keywords: plasmin, multiple myeloma, microenvironment, fibrinolysis

1. Introduction

Multiple Myeloma (MM) is characterized by uncontrolled proliferation of monoclonal plasma cells in the bone marrow (BM) [1,2]. Patients with MM are at increased risk of thrombosis that becomes more prominent after the start of chemotherapy treatment [3,4,5].

The fibrinolytic system is involved in cancer progression [6,7]. The fibrinolytic factor plasminogen (Plg) can be converted into plasmin (Plm) by urokinase or tissue-type plasminogen activators (uPA and tPA, respectively) or kallikrein. At the same time, the activity of uPA and tPA is controlled by Plg activator inhibitors (PAI)-1 and -2. The interaction between cancer cells and stromal fibroblasts can activate the uPA/Plm cascade [8]. Plm inhibition enhanced apoptosis in the M1 melanoma cell line, human HT29 colon carcinoma cell line, and T cell lymphoma [9,10].

High uPA and uPA receptor (uPAR) expressions in MM cells from MM patients were associated with poor prognosis and early extramedullar MM infiltration in patients [3,11,12]. Plm can activate or inactivate chemo-/cytokines (e.g. fibroblast growth factor-2, vascular endothelial growth factor-A, chromogranin A) that are linked to neoangiogenesis in MM [13,14,15,16]. However, the role of fibrinolytic factors in MM cell growth *in vivo* is not well understood.

2. Materials and methods

2.1. Reagents

The Plm inhibitor YO-2 [*trans*-4-aminomethylcyclohexanecarbonyl- Tyr(*O*-Pic)-octylamide] [17,18], from Yoshio Okada (Kobe Gakuin University) was dissolved in PBS or 0.9% NaCl/DMSO (9:1). Bortezomib (BTZ, Cell Signaling Technology) was dissolved in DMSO. Viviren™ In Vivo *Renilla* Luciferase (Promega) working concentration was 0.1 μg/μl of Viviren™ with 100 μl/mouse).

2.2. Mice

Animal procedures were approved by the Experimental Animal Care and Use Committee in the Animal Review Board of Institute of Medical Science, University of Tokyo. 6-8 week-old female CBF1 (Slc:CBF1, $H2k^{b/d}$) female mice were purchased from Japan SLC Inc. 6-8 week-old female NOD/SCID mice were used in this experiment.

2.3. Cell lines

B53, a murine plasmacytoma cell line ($H\text{-}2k^{d}$; provided by Ko Okumura, Juntendo University School of Medicine, Japan) [19] and *Renilla* Luciferase labeled RPMI8226 cells (provided by Muneyoshi Futami, The University of Tokyo, Japan) were cultured in RPMI-1640 medium containing 10% FBS and 1% penicillin/streptomycin.

2.4. Cell proliferation assay and Drug sensitivity testing in vitro

Human RPMI8226 (1 x 10^5 cells/ml/well), and murine hybridoma B53 cells (1 × 10^5 cells/ml/well) were cultured in the presence of YO-2 for 24 hours. Trypan blue exclusion test was used to determine the cell viability. The chemosensitivity of cultured B53 cells for BTZ and doxorubicin (DOX) was tested after 24 hours of incubation. The 50% inhibitory concentration (IC_{50}) per cell type and drug was determined.

2.5. In vivo myeloma mouse model

B53 or RPMI8226 cells were collected, washed twice, and resuspended in PBS or FBS-free RPMI-1640. After cell filtration (40 μM nylon strainer (BD Falcon) cell preparations exceeded 90% viability by trypan blue dye exclusion.

Subcutaneous xenograft model: The dorsal skin of mice was shaved one day before tumor cell inoculation (day -1). The following day (day 0), *Renilla* Luciferase labeled RPMI8226 cells (1 or 4 x 10^6 RPMI8226 cells) were injected subcutaneously into NOD/SCID mice.

Intravenous syngeneic B53 model: CBF1 mice were injected intravenously with 10^6 B53 cells/ CBF1 mouse.

In vivo drug administration: MM cell-inoculated mice were injected every other day with YO-2 at indicated concentration.

2.6. Tumor load evaluation

Tumor length, width, and height were measured by a vernier caliper and the tumor volume was calculated using the following equation [(length) x $(width)^2$]/2. Moreover, the tumor load was determined by measuring the luciferase signal using *in vivo* bioluminescence imaging.

2.7. In vivo bioluminescence imaging

NOD-SCID mice were injected with RMPI8226 cells subcutaneously for bioluminescence imaging. Anesthetized mice (isoflurane, Pfizer) were injected intravenously with 10 μg of Viviren™ In Vivo *Renilla* Luciferase substrate. Tumors were imaged at indicated time points. Using an IVIS® Imaging System 100 Series (Xenogen corporation), images were acquired using a ≤60 second exposure time. The luciferase signal intensity was quantified using region of interest (ROI) (total flux, p/s) with Living Image® 2.50.1 software.

2.8. Survival rate

Mouse survival was monitored on a daily basis. Mice were killed according to animal protection rules. Kaplan-Meier estimates were used to calculate survival rates.

2.9. ELISA

Anti-dinitrophenyl (DNP) Immunoglobulin E (IgE) antibody (Alpha Diagnostic

International), Plasmin-α2 anti-plasmin complex (PAP) (CUSABIO) levels were measured in blood samples using ELISA kits according to the manufacturer's recommendations.

2.10. Organ infiltration

MM cell organ infiltration was determined in femur, tibiae, spleen and liver tissues at indicated time points. Paraffin blocks were prepared from femurs, spleen and liver tissues. Femurs were flushed out to determine the total number of BMMNCs. BMMNCs were stained with FITC-anti-mouse $H2k^d$ (Biolegend), PE-anti-mouse $H2k^b$ (BD Pharmingen), and APC-anti-mouse CD138 (syndecan-1) (Biolegend) at 4°C for 30 minutes. Dead cells were excluded according to PI positivity. Cells were analyzed using a FACSVerse™ flow cytometry. BMMNCs from femur were also used for mRNA extraction.

2.11. RT-PCR

RNA was extracted using TRIzol (Life technology, USA). cDNA was generated using a High-Capacity cDNA Reverse Transcription Kits (Applied Biosystems). The respective forward and reverse primers used for RT-PCR were as follow "Mouse" GAPDH 5'-TCTTGCTCAGTGTCCTTGCTGGG-3', 5'-TGCGACTTCAACAGCAACTCCC AC-3'; uPA 5'-GTCCTCTCTGCAACAGAGTC-3', 5'-CTGTGTCTGAGGGTAATG CT-3'; tPA 5'-GTACTGCTGCTTTGTGGACT-3', 5'-TGCTGTTGGTAAGTTGTC TG-3'; uPAR

5’-TCTGGATCTTCAGAGCTTTC-3’, 5’-AGCACATCTAAGCCTGTA GC-3’; PAI-1 5’-AAAGGACTCTATGGGGAGAA-3’, 5’-TAGGGAGGAGGGAGTT AGAC-3’.

2.12. Statistics

Survival curves were plotted using Kaplan-Meier estimates. Data are reported as the mean ± standard error of the mean (SEM). The Student’s *t*-test was used for statistical analysis of the remaining data. $p<0.05$ was considered statistically significant.

3. Results

3.1. Circulating plasmin is not detectable in subcutaneous (s.c.) xenograft MM mice

Previous studies have shown that patients with myeloma have a decreased fibrinolytic activity [3]. uPA or tPA mRNA was not detected in cells by quantitative PCR (data not shown). To investigate whether Plm activation occurs *in vi*vo, NOD-SCID mice were inoculated with luciferase-tagged RPMI8226 cells (Fig. 1A). Tumor growth was confirmed by manual measurement (Fig. 1B) and by the luciferase signal (Fig. 1C). PAP plasma levels, used as an indicator of active Plm, were not detectable in RPMI8266 tumor-bearing mice by day 20 (Fig. 1D).

3.2. B53 cells express fibrinolytic factors and response to the common MM drugs

Among murine plasmacytoma cell lines tested, B53 cells showed the gene expression of uPA, uPAR and PAI-1, which was reported in primary human MM cells[12] (Fig. 2A). B53 cell proliferation was blocked in cultures supplemented with the common anti-MM drugs BTZ and DOX (Fig. 2B and 2C). When compared to RPMI8226 cells, B53 cells were responsive to these tested MM drugs. So, this cell line was chosen for further analysis.

3.3. Fulminant syngeneic murine MM B53 model with bone marrow engraftment

Bone marrow (BM) cell infiltration is a major clinical feature in MM patients, and stromal cells are a rich source of fibrinolytic factors [20]. Very few MM murine models show MM cell homing to the BM. By injecting B53 cells intravenously into CBF1 mice, we established a fulminant MM model. Tumor cells routinely infiltrated the BM as determined on H&E-stained femur sections (Fig. 3A), and by FACS using $H2K^{d}$ $H2K^{b}$ CD138 staining to discriminate B53 ($H2K^{d+}$ and $CD138^{+}$) from host plasma cells ($H2K^{b+}$ and $CD138^{+}$) (Fig. 3B). Concomitant with the MM cell infiltration into the BM, the total number of BMMNCs decreased (Fig. 3C). Histological analysis of the spleen and liver on day 20 showed massive infiltration of B53 cells with the formation of large tumor nodules (Fig. 3D and E).

B53 cells secrete the paraprotein anti-DNP IgE that can be used to determine the tumor load. Elevated plasma levels of IgE, a oaraprotein secreted by B53 cells were detectable in B53 cell injected mice by day 20, indicating disease progression (Fig. 3F). All B53-injected mice

succumbed by around day 33 (Fig. 3G).

3.4. Plm is dispensable for MM cell progression in the syngeneic B53 MM model

PAP plasma levels were increased in syngeneic intravenously injected B53 MM mice (Fig. 4A). YO-2 blocks the catalytic site of plasmin and inhibits circulating plasmin [15]. YO-2 controls inflammation, and T cell lymphoma growth in mice [10,21,22,23]. To determine the physiological significance of Plm elevation for the survival of B53 bearing mice, mice received intraperitoneal injections of YO-2 daily starting from the day of B53 cell inoculation. We established a maximum tolerated YO-2 dose for 3.75 mg/kg of body weight. YO-2 treatment reduced circulating PAP (Fig. 4A). However, YO-2 treatment did not inhibit tumor progression as indicated by (1) a similar increases in IgE in YO-2- and vehicle-treated groups (Fig. 4B). (2) a similar reduction in the number of BMMNCs (Fig. 4C), (3) a similar percentage of MM cells infiltrating the BM as determined by FACS (Fig. 4D; data of vehicle group shown before in Fig. 3B) and (4) survival rate (Fig. 4E).

While the Plm inhibitor YO-2 prevents the enzymatic action of Plm, the Plm inhibitor tranexamic acid (TA) prevents the conversion of Plg into Plm following binding to generated fibrin [24]. TA also could not prevent tumor growth and progression (data not shown). These data indicate that although Plm activation accompanies MM progression, Plm inhibition could not slow down MM disease progression.

4. Discussion

Fibrinolytic factors have been linked to disease progression in solid and hematological cancers, but their roles in MM are not well understood. Following *in vitro* and *in vivo* studies using a cell line called B53, we demonstrated that plasmin is activated during disease progression. Pharmacological Plm inhibition by YO-2 reduced circulating Plm, but did not change MM cell growth *in vivo* at doses shown to control solid tumor growth in other murine cancers or inflammatory disease models [10,21,22,23]. Our data are in contrast to assumptions made on the effect of the fibrinolytic system in humans: It was reported that patients with myeloma have a decreased fibrinolytic activity mainly because of increased PAI-1 activity [5]. Increased PAI-1 levels have been reported in patients with newly diagnosed MM and correlated with poor prognosis in MM patients [25]. In MM, increased PAI-1 activity seems to be related with elevated IL-6 level. According to these studies one would have expected that plasmin inhibition would worsen the disease progression. But this was not the case.

In the current study, we established a fulminant MM model with high BM homing efficiency by injecting B53 cells intravenously. This B53 MM model showed several important benefits compared to other mouse MM models. The primary benefit for this model is its ability to replicate crucial features of human MM and MM pathogenesis not always seen in other mouse MM models. For example, the homing and infiltration of B53 cells to the BM and

extramedullar organs. One other example was a decrease in BM cellularity observed in B53 injected mice, indicating that B53 cell expansion in BM had affected normal blood cell proliferation, a well-known phenomenon found in MM patients. Therefore, the murine B53 MM model represents an attractive model to study the interaction of myeloma cells with BM stromal cells or MM infiltration. Another benefit of the adjusted model is that the mice do not require irradiation, and thus the MM recipients are immune-competent mice allowing us to study the effects of MM cell growth on immune cells [5]. A further benefit is avoiding problems related to cross-species models due to the syngeneic nature of the new model design. It is also an ideal mouse model for pre-clinical drug testing, because of two main reasons. The disease progresses quickly after initial tumor cell inoculation, and disease progression can be monitored by parameters like circulating IgE levels and mouse survival [26].

Taken together, although plasmin has been suggested to be a driver for MM progression by various other research groups, mostly through *in vitro* studies, here we demonstrate that neither the suppression of plasmin generation nor the inhibition of plasmin alters MM progression *in vivo*.

Acknowledgements. Grant support.

We thank Robert Whittier, Shiou-Yuh Lin, and Kengo Shibata for kindly providing editorial

assistance to the authors during the preparation of this manuscript. We thank Muneyoshi Futami for the *Renilla* Luciferase labeled RPMI8226 cells, Takahiro Kuchimaru for x-ray, and other members of the Stem Cell Dynamics laboratory for helpful discussions and/or experimental assistance. This work was supported in part by grants from the Japan Society for the Promotion of Science (Kiban C grant no. 16K09821, B.H.; grant no. 26461415, K.H), Health and Labour Sciences Research Grants (grant no. 24008, K.H), Mitsubishi Pharma Research Foundation (K.H), Naito Grant (B.H.), and by the collaborative research fund program for women researchers from the Tokyo Medical and Dental University, funded by the "Initiative for Realizing Diversity in the Research Environment", from MEXT, Japan.

Conflict of Interest The authors declare no conflict of interest.

References

[1] A. Palumbo, K. Anderson, Multiple myeloma, N Engl J Med 364 (2011) 1046-1060.

[2] A. Balakumaran, P.G. Robey, N. Fedarko, O. Landgren, Bone marrow microenvironment in myelomagenesis: its potential role in early diagnosis, Expert Rev Mol Diagn 10 (2010) 465-480.

[3] M. Yagci, G.T. Sucak, R. Haznedar, Fibrinolytic activity in multiple myeloma, Am J Hematol 74 (2003) 231-237.

[4] A. Undas, L. Zubkiewicz-Usnarska, G. Helbig, D. Woszczyk, J. Kozinska, A. Dmoszynska, M. Podolak-Dawidziak, K. Kuliczkowski, Altered plasma fibrin clot properties and fibrinolysis in patients with multiple myeloma, Eur J Clin Invest 44 (2014) 557-566.

[5] K. Gado, S. Silva, K. Paloczi, G. Domjan, A. Falus, Mouse plasmacytoma: an experimental model of human multiple myeloma, Haematologica 86 (2001) 227-236.

[6] B. Heissig, D. Dhahri, S. Eiamboonsert, Y. Salama, H. Shimazu, S. Munakata, K. Hattori, Role of mesenchymal stem cell-derived fibrinolytic factor in tissue regeneration and cancer progression, Cell Mol Life Sci 72 (2015) 4759-4770.

[7] B. Heissig, S. Eiamboonsert, Y. Salama, H. Shimazu, D. Dhahri, S. Munakata, Y. Tashiro, K. Hattori, Cancer therapy targeting the fibrinolytic system, Adv Drug Deliv Rev 99 (2016) 172-179.

[8] Y. He, X.D. Liu, Z.Y. Chen, J. Zhu, Y. Xiong, K. Li, J.H. Dong, X. Li, Interaction between

cancer cells and stromal fibroblasts is required for activation of the uPAR-uPA-MMP-2 cascade in pancreatic cancer metastasis, Clin Cancer Res 13 (2007) 3115-3124.

[9] Y. Okada, Y. Tsuda, M. Tada, K. Wanaka, U. Okamoto, A. Hijikata-Okunomiya, S. Okamoto, Development of potent and selective plasmin and plasma kallikrein inhibitors and studies on the structure-activity relationship, Chem Pharm Bull (Tokyo) 48 (2000) 1964-1972.

[10] M. Ishihara, C. Nishida, Y. Tashiro, I. Gritli, J. Rosenkvist, M. Koizumi, Y. Okaji, R. Yamamoto, H. Yagita, K. Okumura, M. Nishikori, K. Wanaka, Y. Tsuda, Y. Okada, H. Nakauchi, B. Heissig, K. Hattori, Plasmin inhibitor reduces T-cell lymphoid tumor growth by suppressing matrix metalloproteinase-9-dependent CD11b(+)/F4/80(+) myeloid cell recruitment, Leukemia 26 (2012) 332-339.

[11] G.M. Rigolin, A. Tieghi, M. Ciccone, L.Z. Bragotti, F. Cavazzini, M. Della Porta, B. Castagnari, R. Carroccia, G. Guerra, A. Cuneo, G. Castoldi, Soluble urokinase-type plasminogen activator receptor (suPAR) as an independent factor predicting worse prognosis and extra-bone marrow involvement in multiple myeloma patients, Br J Haematol 120 (2003) 953-959.

[12] O. Hjertner, G. Qvigstad, H. Hjorth-Hansen, C. Seidel, J. Woodliff, J. Epstein, A. Waage, A. Sundan, M. Borset, Expression of urokinase plasminogen activator and the urokinase plasminogen activator receptor in myeloma cells, Br J Haematol 109 (2000) 815-822.

[13] B. Cauwe, P.E. Van den Steen, G. Opdenakker, The biochemical, biological, and pathological

kaleidoscope of cell surface substrates processed by matrix metalloproteinases, Crit Rev Biochem Mol Biol 42 (2007) 113-185.

[14] B. Heissig, M. Ohki-Koizumi, Y. Tashiro, I. Gritli, K. Sato-Kusubata, K. Hattori, New functions of the fibrinolytic system in bone marrow cell-derived angiogenesis, Int J Hematol 95 (2012) 131-137.

[15] E. Lee, R. Enomoto, K. Takemura, Y. Tsuda, Y. Okada, A selective plasmin inhibitor, trans-aminomethylcyclohexanecarbonyl-L-(O-picolyl)tyrosine-octylamide (YO-2), induces thymocyte apoptosis, Biochemical Pharmacology 63 (2002) 1315-1323.

[16] M. Bianco, A.M. Gasparri, B. Colombo, F. Curnis, S. Girlanda, M. Ponzoni, M.T.S. Bertilaccio, A. Calcinotto, A. Sacchi, E. Ferrero, M. Ferrarini, M. Chesi, P.L. Bergsagel, M. Bellone, G. Tonon, F. Ciceri, M. Marcatti, F. Caligaris-Cappio, A. Corti, Chromogranin A Is Preferentially Cleaved into Proangiogenic Peptides in the Bone Marrow of Multiple Myeloma Patients, Cancer Res 76 (2016) 1781-1791.

[17] R. Enomoto, C. Sugahara, T. Komai, C. Suzuki, N. Kinoshita, A. Hosoda, A. Yoshikawa, Y. Tsuda, Y. Okada, E. Lee, The structure-activity relationship of various YO compounds, novel plasmin inhibitors, in the apoptosis induction, Biochimica Et Biophysica Acta-General Subjects 1674 (2004) 291-298.

[18] Y. Tsuda, M. Tada, K. Wanaka, U. Okamoto, A. Hijikata-Okunomiya, S. Okamoto, Y. Okad, Structure-inhibitory activity relationship of plasmin and plasma kallikrein inhibitors,

Chem Pharm Bull (Tokyo) 49 (2001) 1457-1463.

[19] I. Bottcher, M. Ulrich, N. Hirayama, Z. Ovary, Production of monoclonal mouse IgE antibodies with DNP specificity by hybrid cell lines, Int Arch Allergy Appl Immunol 61 (1980) 248-250.

[20] D. Dhahri, K. Sato-Kusubata, M. Ohki-Koizumi, C. Nishida, Y. Tashiro, S. Munakata, H. Shimazu, Y. Salama, S. Eiamboonsert, H. Nakauchi, K. Hattori, B. Heissig, Fibrinolytic crosstalk with endothelial cells expands murine mesenchymal stromal cells, Blood 128 (2016) 1063-1075.

[21] B. Szende, Y. Okada, Y. Tsuda, A. Horvath, G. Bokonyi, S. Okamoto, K. Wanaka, G. Keri, A novel plasmin-inhibitor inhibits the growth of human tumor xenografts and decreases metastasis number, In Vivo 16 (2002) 281-286.

[22] A. Sato, C. Nishida, K. Sato-Kusubata, M. Ishihara, Y. Tashiro, I. Gritli, H. Shimazu, S. Munakata, H. Yagita, K. Okumura, Y. Tsuda, Y. Okada, A. Tojo, H. Nakauchi, S. Takahashi, B. Heissig, K. Hattori, Inhibition of plasmin attenuates murine acute graft-versus-host disease mortality by suppressing the matrix metalloproteinase-9-dependent inflammatory cytokine storm and effector cell trafficking, Leukemia 29 (2015) 145-156.

[23] S. Munakata, Y. Tashiro, C. Nishida, A. Sato, H. Komiyama, H. Shimazu, D. Dhahri, Y. Salama, S. Eiamboonsert, K. Takeda, H. Yagita, Y. Tsuda, Y. Okada, H. Nakauchi, K.

Sakamoto, B. Heissig, K. Hattori, Inhibition of plasmin protects against colitis in mice by suppressing matrix metalloproteinase 9-mediated cytokine release from myeloid cells, Gastroenterology 148 (2015) 565-578 e564.

[24] L. Tengborn, M. Blomback, E. Berntorp, Tranexamic acid--an old drug still going strong and making a revival, Thromb Res 135 (2015) 231-242.

[25] M. Misiewicz, M. Robak, K. Chojnowski, J. Trelinski, [Correlations between ROTEM fibrinolytic activity and t-PA, PAI-1 levels in patients with newly diagnosed multiple myeloma], Pol Merkur Lekarski 36 (2014) 316-319.

[26] R.A. Fryer, T.J. Graham, E.M. Smith, S. Walker-Samuel, G.J. Morgan, S.P. Robinson, F.E. Davies, Characterization of a novel mouse model of multiple myeloma and its use in preclinical therapeutic assessment, PLoS One 8 (2013) e57641.

Figure legends

Fig. 1. **No circulating plasmin detectable in NOD/SCID mice after subcutaneous injection of human RPMI8226 cells.** 1-4 x 10^6 *Renilla* Luciferase labeled RPMI8226 human myeloma cells were injected subcutaneously into NOD/SCID mice (n=6/group). (A) Tumor size was measured at indicated time points. (B) A photomontage of representative images of tumor load was determined by the mean luminescence. (C) Murine Plasmin α2 anti-plasmin (PAP) (n=2-3) in plasma levels at indicated times.

Fig. 2. **B53 plasmacytoma cells show similar expression of fibrinolytic factors and responses to MM common drugs.** (A) Mouse urokinase plasminogen activator (*uPA*) and tissue type plasminogen activator (*tPA*), plasminogen activator inhibitor-1 (*PAI-1*), and uPA receptor (*uPAR*) gene expression was tested in B53 cells by quantitative real-time PCR (n=3). B53 cells were treated with (B) bortezomib (BTZ) or (C) doxorubicin (DOX). Cell viability was determined by trypan exclusion (n=3/group). Data are represented as mean ± SEM. *, + $p<0.05$, **, ++ $p<0.02$ when compared to control. Data are shown as a representative of at least two independent experiments with similar results.

Fig. 3. **Myeloma cell infiltrated the bone marrow and soft tissue of B53 cell-injected mice.** CBF1 mice were intravenously inoculated with 1 × 10^6 B53 cells. (A) Representative

H&E stained bone marrow (BM) sections of mice day 20 after B53 injection showing massive MM cell infiltration (yellow dotted line, Scale bars; 20μm). (B) BMMNCs were stained with the MM cell expressing markers CD138 and $H2k^d$ and analyzed by FACS (n=8-10) and (C) the number of BMMNCs were manually counted at day 20 after B53 injection (n=3-5). Data are represented as mean ± SEM. ** $p<0.02$ when compared to control. (D-E) Pathology of spleen and liver showed B53 infiltration (yellow dotted line) by H&E staining (Scale bars; 20μm). (F) Plasma anti-dinitrophenyl Immunoglobulin E (anti-DNP-IgE) levels in the plasma at day 0 and at day 20 of B53-bearing mice (n=3-5/group). Data are represented as mean ± SEM. ** $p<0.02$ when compared to control. (G) Kaplan-Meier survival curve of B53 injected mice (n=10). N.S., not significant.

Fig. 4. **Plasmin inhibition cannot delay tumor progression in murine B53 multiple myeloma model.** 1×10^6 B53 cells were intravenously injected into CBF1 mice. (A) Murine PAP (n=10-16) in plasma levels at indicated times. (B) Plasma anti-dinitrophenyl Immunoglobulin E (anti-DNP-IgE) concentration was measured at indicated days by ELISA (n=3-8). Data are represented as mean ± SEM. * $p<0.05$, ** $p<0.02$ when compared to control. (C) Number of BMMNCs was manually counted at indicated time points per femur (n=8-10/group). Data are represented as mean ± SEM. * $p<0.05$, ** $p<0.02$ when compared to control. (D) BM infiltration of B53 myeloma cells was determined by FACS after staining

with antibodies against $CD138^{+}H2K^{d+}$ cells (n=9 for YO-2-treated cancer bearing mice). Data are represented as mean ± SEM. ** $p<0.02$. (E) Kaplan-Meier survival curve of B53 myeloma mice treated with 3.75 mg/kg (n=33) of YO-2, or treated with carrier (n=23). Data are shown as mean ± SEM. N.S., not significant when compared to control.

Figure 1

Eiamboonsert et al.

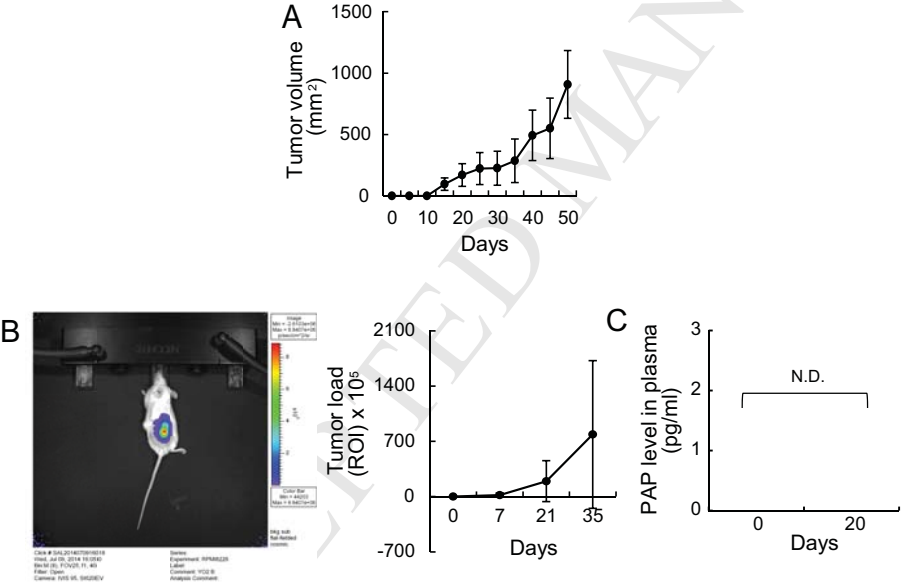

Figure 2

Eiamboonsert et al.

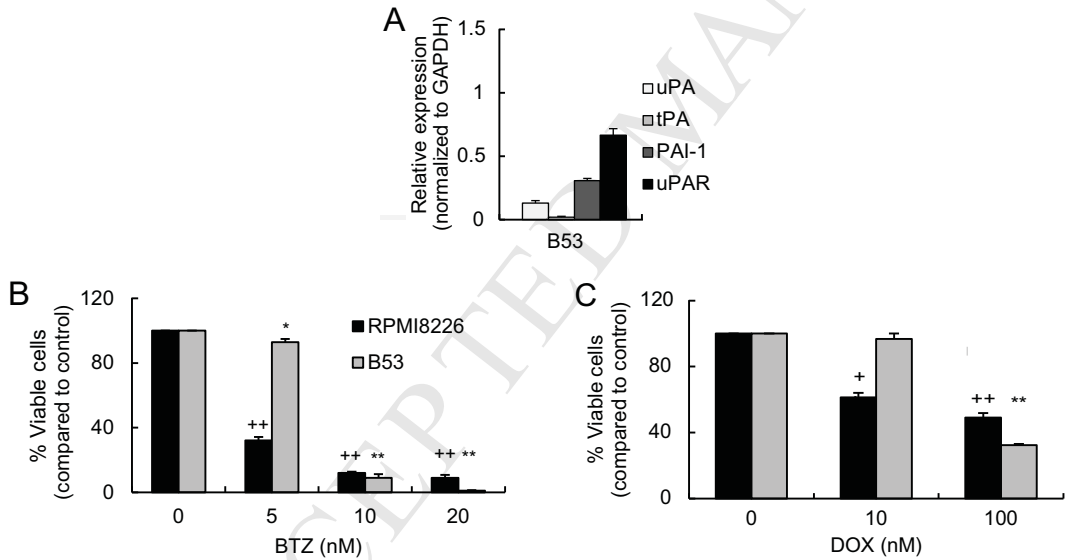

Figure 3

Eiamboonsert et al.

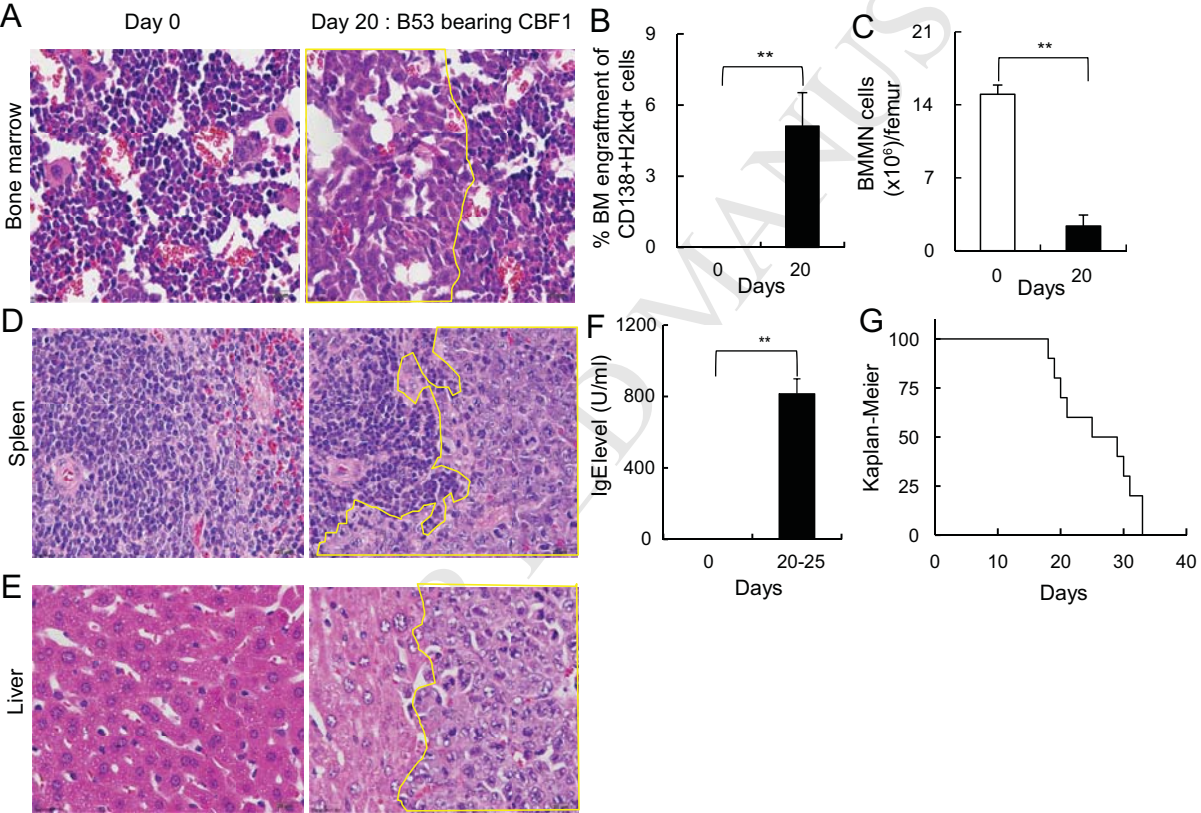

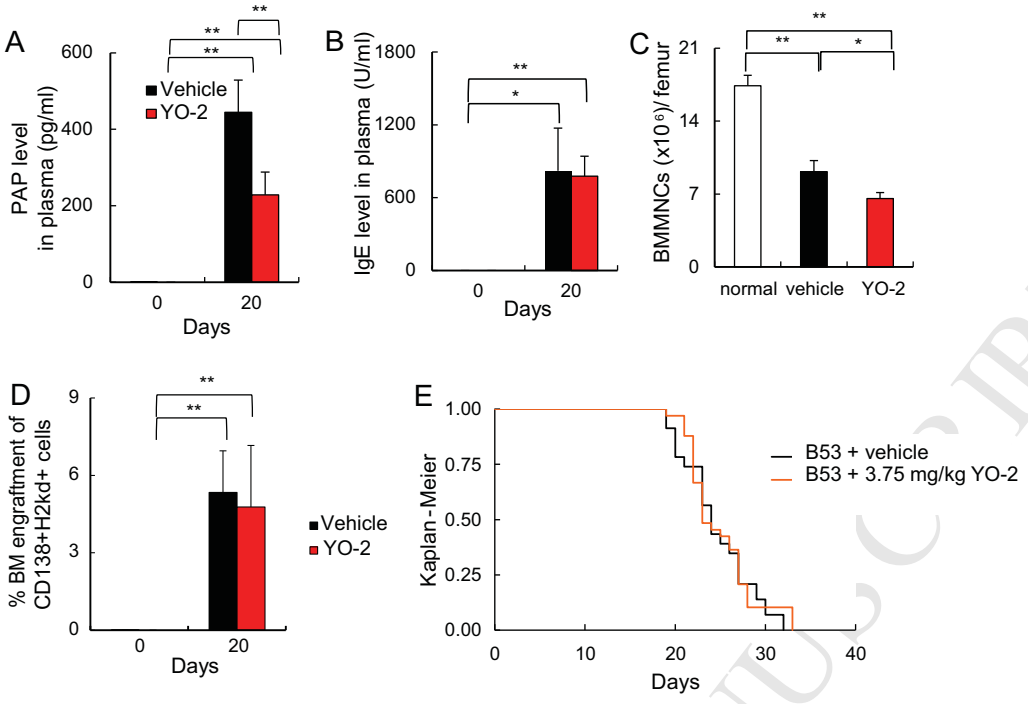

Highlights

Eiamboonsert et al. "**The role of plasmin in the pathogenesis of murine multiple myeloma"**

- We established a murine model for multiple myeloma (MM) using the murine plasmacytoma cell line B53 that shows bone marrow infiltration and extramedullar cell growth.
- Fibrinolytic factor expression (like urokinase or tissue type plasminogen activator, and its endogenous inhibitor PAI-1) in B53 cells was similar to the expression pattern reported for primary human MM cells.
- Systemic increases in Plm, although occurring *in vivo*, did not alter MM disease progression as demonstrated using two different Plm inhibitors.